

THE LANCET

Supplementary appendix 1

This appendix formed part of the original submission and has been peer reviewed. We post it as supplied by the authors.

Supplement to: lungman T, Cirach M, Marando F, et al. Cooling cities through urban green infrastructure: a health impact assessment of European cities. *Lancet* 2023; published online Jan 31. [https://doi.org/10.1016/S0140-6736\(22\)02585-5](https://doi.org/10.1016/S0140-6736(22)02585-5).

**COOLING CITIES FOR HEALTH THROUGH GREEN INFRASTRUCTURE:
A HEALTH IMPACT ASSESSMENT FOR EUROPEAN CITIES**

Tamara lungman^{1,2,3}, Marta Cirach^{1,2,3}, Federica Marando⁴, Evelise Pereira Barboza^{1,2,3}, Sasha Khomenko^{1,2,3}, Pierre Masselot⁵, Marcos Quijal-Zamorano^{1,2}, Natalie Mueller^{1,2,3}, Antonio Gasparrini^{5,6,7}, José Urquiza^{1,2,3}, Mehdi Heris⁸, Meelan Thondoo^{1,9}, Mark Nieuwenhuijsen^{1,2,3}

1 Institute for Global Health (ISGlobal), Barcelona, Spain

2 Department of Experimental and Health Sciences, Universitat Pompeu Fabra, Barcelona, Spain

3 CIBER Epidemiología y Salud Pública (CIBERESP), Madrid, Spain

4 European Commission – Joint Research Centre, Ispra, Italy

5 Department of Public Health, Environments and Society, London School of Hygiene and Tropical Medicine (LSHTM), London, UK

6 Centre on Climate Change and Planetary Health, London School of Hygiene & Tropical Medicine (LSHTM), London, UK

7 Centre for Statistical Methodology, London School of Hygiene & Tropical Medicine (LSHTM), London, UK

8 Hunter College City University of New York

9 MRC Epidemiology Unit, University of Cambridge School of Clinical Medicine, Cambridge, UK

Correspondence to:

Prof. Mark Nieuwenhuijsen,

ISGlobal, 08003, Barcelona, Spain

mark.nieuwenhuijsen@isglobal.org

Content

List of acronyms	3
Evidence before the study	4
Supplement A. City definition	5
Supplement B. Demographic data	6
Supplement C. Health Impact Assessment (HIA)	9
Supplement D. Exposure Response Function (ERF)	13
Supplement E. Counterfactual scenarios.	18
<i>a) Urban Heat Island (UHI)</i>	18
<i>b) TC 30%</i>	21
Supplementary F. Sensitivity analysis.	27
<i>a) Health impact assessment of urban heat island</i>	27
<i>b) Cooling estimation</i>	30
<i>c) 30% TC health impact assessment</i>	32
Supplementary analysis G. Uncertainty analyses.	35
References	37

List of acronyms

CI	Confidence interval
CRA	Comparative risk assessment
CVD	Cardiovascular disease
ERF	Exposure-response function
ESP	European standard population
Etree	Water evaporated from trees
FUA	European Functional Urban Area
GHSL	Global Human Settlement Layer
HIA	Health impact assessment
LST	Land Surface Temperature
NCD	Non-communicable diseases
NDVI	Normalized difference vegetation index
NUTS	Nomenclature of Territorial Units for Statistics
PAF	Population Attributable Fraction
PML	Penman-Monteith-Leuning
RMSE	Root mean squared error
Tair	Maximum air temperature
TC	Tree cover
UGI	Urban green infrastructure
UHI	Urban heat island
UrbClim	Urban Climate model
WHO	World Health Organization
YLL	Years of Life Lost

Evidence before the study

We did two different literature searches in PubMed, Scopus, and Google Scholar. For the first one, our search terms were: "urban heat island" AND "mortality" OR "premature mortality" AND "impact assessment" OR "health impact". For the second one our search terms were: "green spaces" OR "green areas" OR "urban green infrastructure" OR "tree cover" OR "tree coverage" OR "tree canopy" OR "urban trees" AND "cooling" OR "temperature reduction" OR "heat mitigation" AND "mortality" OR "premature mortality" AND "impact assessment" OR "health impact"

Supplement A. City definition

City definition

We retrieved the European cities from the Urban Audit (UA) 2018 dataset (1). The city definition was based on the presence of an “urban centre”, which is defined as followed: (1) Selection of grid cells with population density over 1,500 inhabitants/km²; (2) Clustering of contiguous high-density cells and selection of clusters with a population above 50,000 inhabitants as the “urban centre”; (3) Defining cities as the local administrative units with at least half their population in an “urban centre”. For urban centres that extends far beyond the city, a ‘greater city’ level was created (2).

Supplement B. Demographic data

a) Population data

The Global Human Settlement Layer (GHSL) method combines information from population censuses and downscales the population into grid cells of 250m by 250m resolution, based on the presence or absence of built-up area in the grid cell (3). We reduced the GHSL reference dataset to only those grid cells that covered residential areas to better represent population distribution, to avoid locating inhabitants in non-residential areas (eg. industrial zones, port areas, airports). We retrieve land use data from the European Urban Atlas 2012 and retain grid cells that intersect with any of the residential categories defined in the Urban Atlas (i.e. Continuous Urban Fabric, Discontinuous Dense Urban Fabric, Discontinuous Medium-Density Urban Fabric, Discontinuous Low-Density Urban Fabric and Discontinuous Very Low-Density Urban Fabric) (4).

Given that the UrbClim data was available at a gridded raster, for some cities the overlap with the Urban Audit layer was not exact and as a result there were city grid-cells with no temperature data which were excluded from the analysis (ie, a city-average equal to 97.7% of population covered) (a full list with the percentage of grids and population covered is available in the Supplementary Table 1).

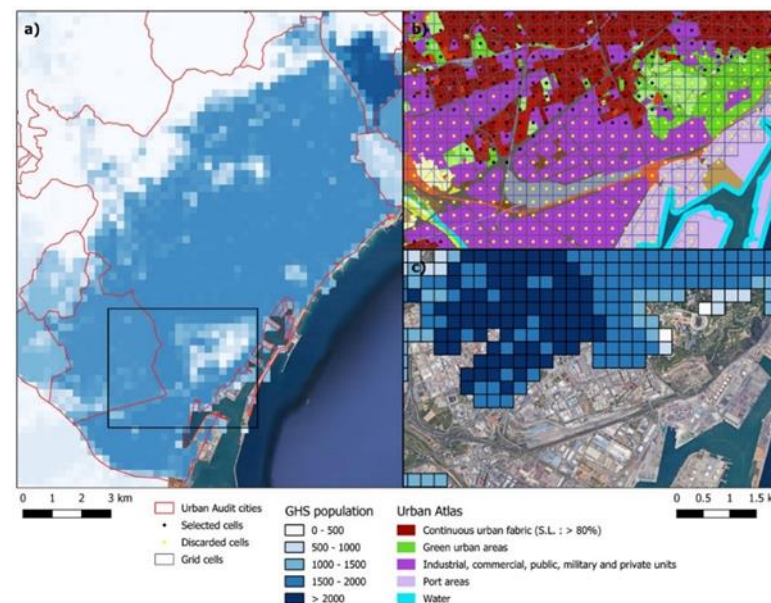


Figure S1: Example of procedure applied for the population redistribution (example: Barcelona area): a) original population raster from GHSL, b) selection of cells based on residential land uses, and c) final dataset with weighted population redistribution assigned for each cell

b) Age distribution

The population age distribution for 2015 was obtained from Eurostat at the Nomenclature of Territorial Units for Statistics (NUTS) 3 level (5,6). We retrieved the population data by age group (i.e. 20-24, 25-29, 30-34, 35-39, 40-44, 45-49, 50-54, 55-59, 60-64, 65-69, 70-74, 75-79, 80-84 and 85 years and older) and calculated the proportion of the population per age group. We assumed the same age distribution between the NUTS3-level and the corresponding city level. The population age proportions of each city were applied to the total population counts in the corresponding grid cells to estimate the population by age group for each grid cell and the city-level adult population count. After that, we aggregated the groups as 20-44, 45-64, 65-74, 75-84 and 85 years and older to fit them with ERFs.

c) Mortality data

We retrieved weekly all-cause mortality counts by age group for 2015 from Eurostat (7) for 81 cities at NUTS3 level. We estimated the daily mortality rates per age group per city assuming an homogeneous distribution of deaths over the same week and applied the rates to each grid cell.

For cities without weekly deaths counts available (ie, Berlin, Dusseldorf, Frankfurt, Hamburg, Koln, Leipzig, Ljubljana, Munich, Prague, Split, Zagreb) we retrieved annual city-specific all-cause mortality counts for 2015 from Eurostat (7). For only one city (ie, Dublin) we estimated the total all-cause mortality count using the country-level age-specific all-cause mortality rates, which was also available through the Eurostat database. We estimated the mortality rates per age group and applied the rates to each grid cell. We retrieved monthly country mortality counts (7) and estimated the proportion of deaths per month. We assumed an homogeneous distribution of deaths over the same month and estimated the daily deaths per grid cell.

For the 81 cities with weekly mortality data, we also retrieved annual city-specific all-cause mortality and followed the same procedure as described before for comparison. On average, the death counts estimated with the annual city-specific dataset were 17% higher with a Pearson correlation equal to 0.98. We ran a linear regression between both data sets (Table S1) and adjusted the annual mortality dataset by applying a calibration of 86%.

		<i>p</i> -value
Intercept	-10.34	0.766
Coefficient	0.86	< 2.2e-16

Table S1. Linear regression coefficients and *p*-values for the association between the annual city-specific dataset and the weekly NUTS3 dataset.

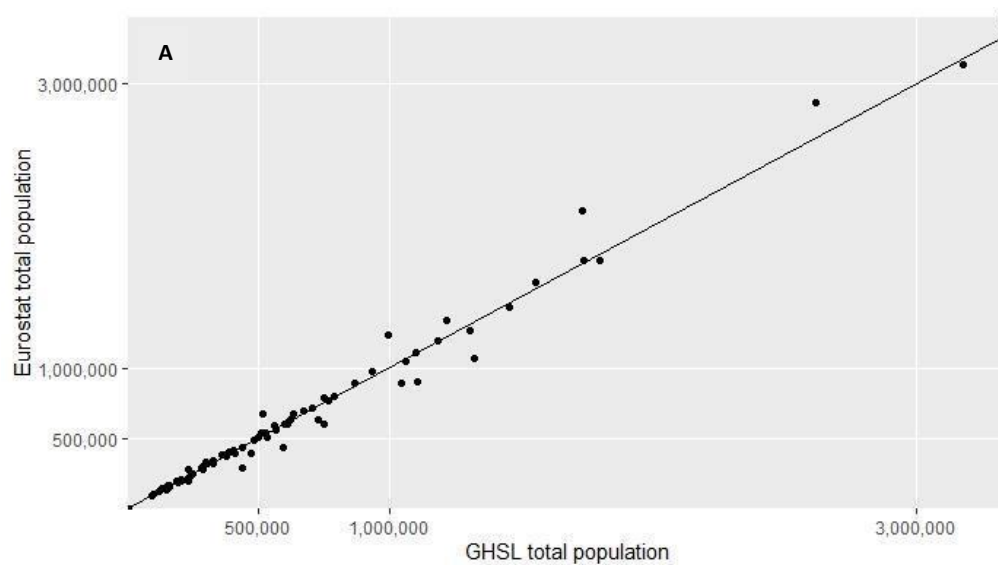
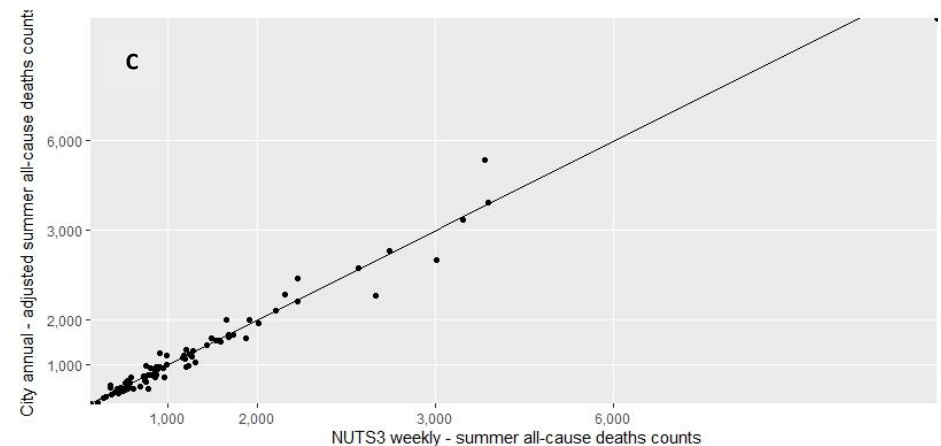
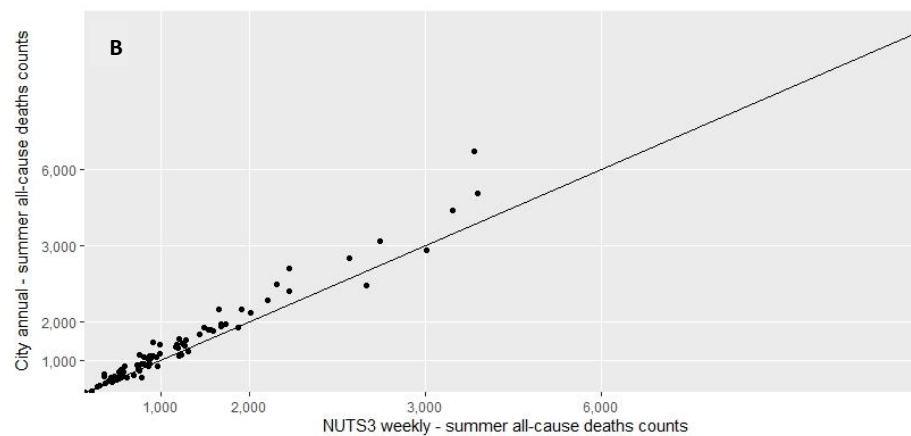


Figure S2: (A) Association between GHSL total population and Eurostat total population. (Pearson correlation=0.99). **(B)** Association between summer all-cause deaths counts estimations from city level annual deaths counts and from NUTS3 level weekly deaths counts. (Pearson correlation=0.98). **(C)** Association between adjusted summer all-cause deaths counts estimations from city level annual deaths counts and from NUTS3 level weekly deaths counts. (Pearson correlation=0.98).



Supplement C. Health Impact Assessment (HIA)

We have analysed the historical average summer temperature according to the Köppen–Geiger climate zones to check whether 2015 was a normal year. We did not identify 2015 as an abnormal temperature year, however we observed an overall light increase trend (Figure S3).

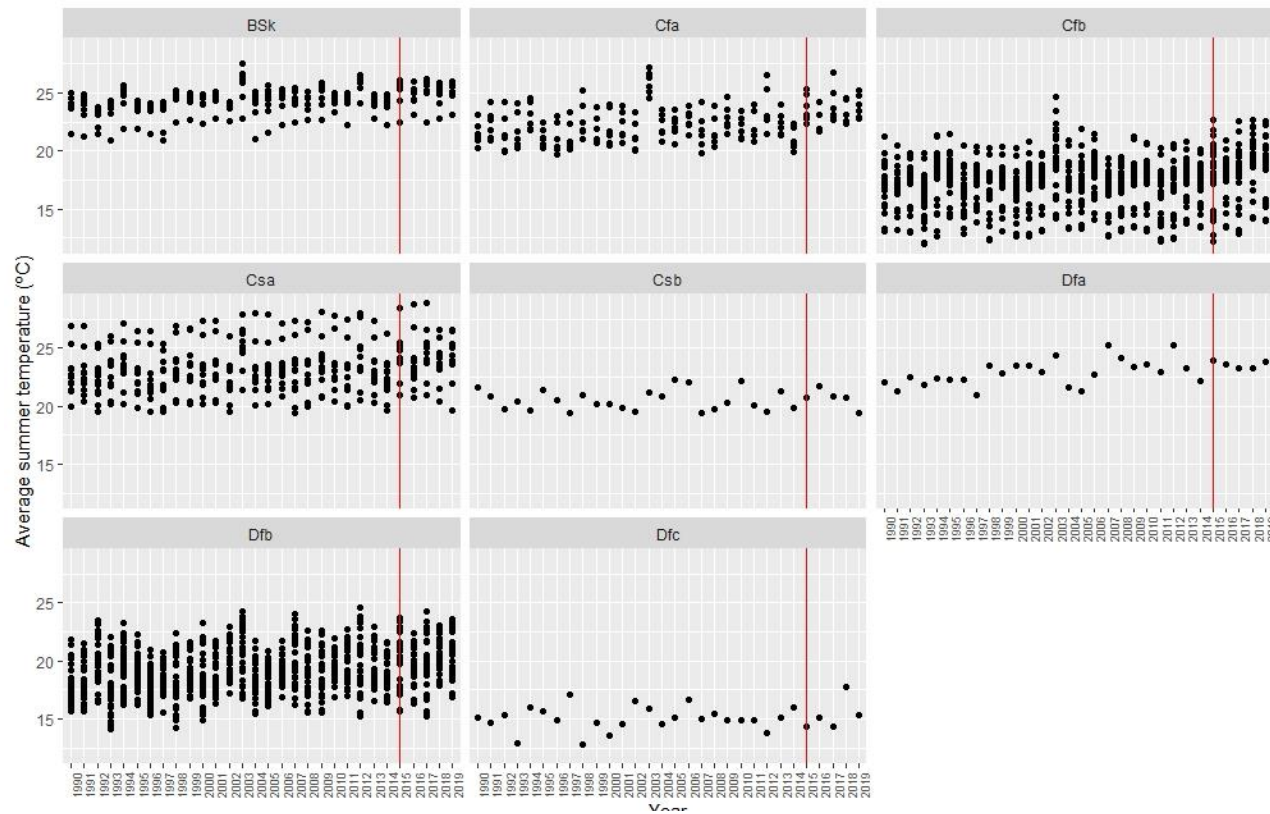


Figure S3. Average summer temperature by climate zone from 1991 to 2019. The red line indicates 2015, the baseline year for the analysis BSk = Arid, steppe, cold; Cfa= Temperate, no dry season, hot summer; Cfb= Temperate, no dry season, warm summer; Csa= Temperate, dry summer, hot summer; Csb= Temperate, dry summer, warm summer; Dfa= Cold, no dry season, hot summer; Dfb= Cold, no dry season, warm summer; Dfc= Cold, no dry season, cold summer

We retrieved city and age group-specific exposure-response functions (ERFs) from Masselot et al 2021 (8). We estimated the daily baseline temperature exposure levels and we assigned to each age group a RR accordingly. We calculated the Population Attributable Fraction (PAF) for each daily mean temperature (i) and age group (j) at a grid-cell level (k) as:

$$\text{Eq. (S2)} \quad \text{PAF}_{ijk} = \frac{\text{RR}_{ijk} - 1}{\text{RR}_{ijk}}$$

The PAF is the proportional reduction in population mortality that would occur if temperature were reduced to the corresponding 'Minimum mortality temperature (MMT)' (ie, the mean daily temperature at which the lowest mortality occurs) (9).

We estimated the attributable premature mortality burden combining the PAF and the daily natural-cause mortality. We repeated the same procedure for each of the counterfactual scenarios and we calculated the difference with the baseline scenario. The obtained result is the premature mortality burden attributed to shifting baseline exposure levels to the specific counterfactual exposure level scenario (Figure S4).

We added up the results by city and age groups and estimated the preventable age-standardized mortality per 100,000 population, based on European Standard Population (ESP) (10) and the percentage of preventable annual and summer all-cause deaths. Additionally, we calculated the Years of Life Lost (YLL) due to the premature deaths as:

$$\text{Eq. (S3)} \quad \text{YLL} = \text{Attributable deaths}_{\text{age group}} * \text{Life expectancy}_{\text{age of death}}$$

YLL is a measure of premature mortality that considers both the frequency of deaths and the age at which it occurs. The YLLs for a cause are essentially calculated as the number of deaths from the specific cause multiplied by a loss function specifying the years lost for deaths as a function of the age at which death occurs. The average age at death was estimated as the mean age of each age group by city and the standard life expectancy at the age of death was obtained from country-level life tables available through Eurostat (11). YLL depends on an age weighting that encodes how the value of life is distributed with age, and on a time discount rate that represents a possible decreasing value of future lives. In this study, we applied a uniform age weighting and a 0%-time discount rate following the GBD and WHO approach to count years lived equally at all ages now and in the future (ie, giving an equal weight to years of

healthy life lost at young ages and older ages) (12). We performed the analysis considering the sources of uncertainty. We built the range of uncertainty for each of the parameters involved in the mortality impacts estimations based on their SE and assuming a normal distribution. We then conducted 500 Monte Carlo iterations by sampling from the built ranges at a grid-cell level. From each sampling we aggregated the results to a city level, therefore we ended up with 500 results for each city, from which we estimated the mean (point estimate) and 2.5 and 97.5 percentiles (95% CI) for each city.

For building the temperature and the UHI uncertainty ranges (both datasets with daily and gridded variability) we considered a sample by day (ie, same error for all of the grids for each day) for avoiding errors from cancelling each other out.

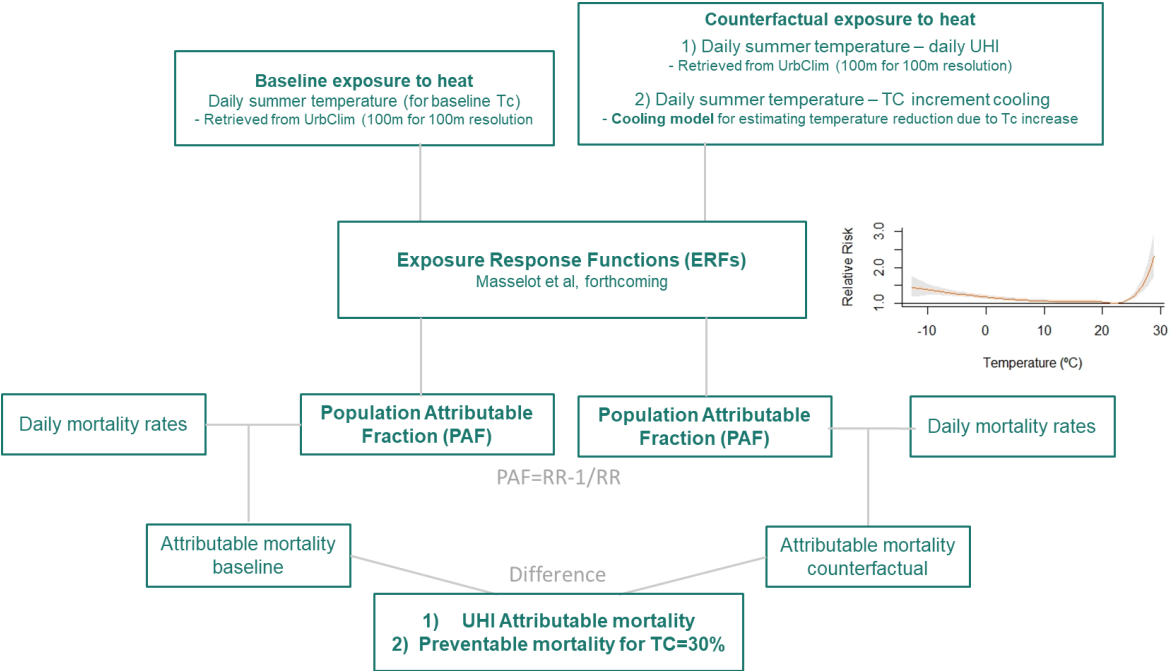
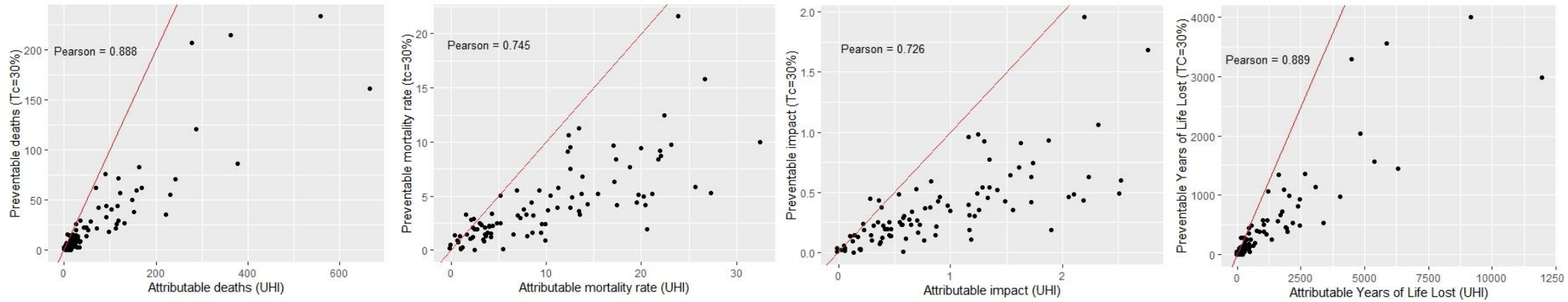


Figure S4. Summarised methodological steps of the Health Impact Assessment analysis.

Association between UHI HIA and TC=30% HIA



Supplement D. Exposure Response Function (ERF)

We generated city and age-specific ERFs from the framework of Masselot et al (forthcoming). The authors developed a three-stage analysis design to map ERFs across Europe. Very briefly, first, they estimated the city-specific overall cumulative exposure-response function in cities with observed daily mortality data through a quasi-Poisson regression model accounting for non-linearity and lagged effects. Secondly, they created a predictive model by conducting a meta-regression of the first-stage ERF coefficients using age, regional indicator and city-specific characteristics. This meta-regression model can then be used to predict ERF for any age group and any city in Europe (1).

Given that the risk estimates were built under the ERA5-LAND temperature dataset with a resolution of approximately 9 km, therefore covering rural areas, it was expected that the ERF temperature range was lower than the UrbClim temperature range. For that reason, we applied a city-specific correction to the UrbClim dataset as:

$$\text{Eq. (S1)} \quad T_{\text{urbclim}} = \alpha + \beta * T_{\text{era5}}$$

Where T_{urbclim} is the mean UrbClim daily city-level temperature and T_{era5} is the mean ERA5-LAND daily city-level temperature for 2015.

We then ran Eq1' at a grid cell-level with their corresponding city-specific coefficients.

$$\text{Eq. (S1')} \quad T_{\text{urbclim adjusted}} = (T_{\text{urbclim}} - \alpha) / \beta$$

Table S2. Statistical distribution of Equation 1 coefficients and determinant coefficient (R^2)

α	β	R^2
-1.22 ± 0.95	-0.98 ± 0.03	0.98 ± 0.01

After adjusting the temperature dataset, there were still some days with temperature values falling out of the ERFs (ie, temperature values above the maximum temperature with an estimated risk). We chose a conservative approach and instead of extrapolating the ERFs above the maximum, we assigned to highest temperatures, the corresponding maximum temperature' risk available (Table S3).

Table S3. Maximum exposure-response function predictive values and maximum UrbClim values at a grid-cell level (250m). Adjustment equation applied to each city.

City name	City code	Maximum ERF predictive values (°C)	Maximum summer temperature UrbClim (250m)	Difference (°C)	Alfa	Beta	error	R squared
Wien	AT001C1	28.885	32.28	3.395	-1.24	1.00	0.90	0.99
Graz	AT002C1	25.559	30.738	5.179	-2.35	1.00	0.76	0.99
Bruxelles / Brussel	BE001C1	26.563	29.928	3.365	-1.22	0.98	0.77	0.98
Antwerpen	BE002C1	26.319	29.095	2.777	-0.84	0.98	0.73	0.98
Gent	BE003C1	26.815	28.863	2.047	-0.30	1.00	0.59	0.99
Charleroi	BE004C1	26.373	29.062	2.689	-0.67	0.97	0.74	0.98
Liège	BE005C1	26.904	31.338	4.433	-0.88	0.98	0.73	0.99
Sofia	BG001C1	31.871	30.58	-1.291	-2.57	1.03	1.03	0.99
Varna	BG003C1	30.402	31.39	0.987	-0.97	0.96	0.75	0.99
Zürich	CH001C1	27.747	32.652	4.906	-1.96	0.96	0.97	0.98
Genève	CH002C1	27.559	31.756	4.196	-3.40	1.04	1.03	0.98
Basel	CH003C1	24.628	32.582	7.954	-3.03	0.99	1.00	0.98
Praha	CZ001C1	28.369	32.19	3.821	-0.62	0.99	0.53	1.00
Berlin	DE001C1	27.598	33.055	5.457	-1.05	0.99	0.74	0.99

Hamburg	DE002C1	26.425	29.404	2.979	-0.52	0.97	0.67	0.99
München	DE003C1	27.548	31.115	3.567	-1.85	0.98	1.28	0.97
Köln	DE004C1	28.414	31.656	3.242	-0.90	0.98	0.52	0.99
Frankfurt am Main	DE005C1	28.861	33.643	4.781	-1.65	0.99	0.90	0.98
Leipzig	DE008C1	29.899	31.544	1.646	-0.50	0.96	0.77	0.99
Düsseldorf	DE011C1	28.448	31.057	2.609	-0.69	0.99	0.54	0.99
København	DK001C1	24.295	28.48	4.185	-0.67	0.96	0.61	0.99
Tallinn	EE001C1	25.308	22.725	-2.583	-0.41	0.99	0.40	1.00
Tartu	EE002C1	25.775	23.979	-1.797	-0.41	0.99	0.40	1.00
Athina	EL001C2	32.653	36.119	3.465	-2.31	0.95	1.32	0.97
Thessaloniki	EL002C2	32.336	33.997	1.661	-2.90	0.98	0.71	0.99
Madrid	ES001C1	26.26	35.15	8.89	-2.74	1.02	1.12	0.98
Barcelona	ES002C1	24.523	31.625	7.102	-2.04	1.00	0.50	0.99
Valencia	ES003C1	24.577	33.633	9.056	-1.97	1.01	0.70	0.99
Sevilla	ES004C1	25.198	35.719	10.521	-1.52	1.01	0.58	0.99
Málaga	ES006C1	26.504	36.295	9.791	-1.50	0.94	0.54	0.99
Murcia	ES007C1	27.01	34.025	7.015	-0.40	0.95	0.45	1.00
Palma de Mallorca	ES010C1	23.231	31.785	8.554	-0.11	0.96	0.56	0.99
Bilbao	ES019C1	28.18	28.813	0.633	-0.10	0.91	0.61	0.98
Alicante/Alacant	ES021C1	31.628	32.547	0.919	0.38	0.94	0.57	0.99
Helsinki / Helsingfors	FI001C2	24.962	23.247	-1.715	-1.59	1.01	0.74	0.99
Paris	FR001C1	28.49	33.547	5.057	-2.75	0.99	1.13	0.97
Lyon	FR003C2	28.486	33.971	5.485	-2.12	1.02	0.96	0.98
Toulouse	FR004C2	29.287	30.758	1.472	-0.81	1.00	0.66	0.99
Strasbourg	FR006C2	27.683	35.122	7.44	-2.27	1.00	0.68	0.99
Bordeaux	FR007C1	30.57	32.196	1.626	-1.06	1.00	0.57	0.99
Nantes	FR008C1	28.628	29.779	1.15	0.02	0.96	0.53	0.99
Lille	FR009C1	29.83	29.613	-0.218	-0.76	0.99	0.67	0.99

Montpellier	FR010C1	29.54	31.038	1.498	0.03	0.96	0.46	0.99
Marseille	FR203C1	30.115	30.696	0.581	0.03	0.94	0.54	0.99
Nice	FR205C2	27.434	33.97	6.536	-1.80	0.98	0.59	0.99
Zagreb	HR001C1	29.878	32.442	2.564	-1.11	0.99	0.62	0.99
Split	HR005C1	28.599	33.525	4.926	-1.72	0.96	0.62	0.99
Budapest	HU001C1	29.493	33.713	4.22	-1.51	0.99	0.84	0.99
Miskolc	HU002C1	29.547	33.466	3.919	-1.54	0.96	0.79	0.99
Pécs	HU004C1	28.859	31.722	2.863	-0.34	0.98	0.48	1.00
Debrecen	HU005C1	28.734	31.762	3.028	-0.07	0.98	0.43	1.00
Szeged	HU006C1	28.664	33.782	5.118	-0.77	0.97	0.70	0.99
Győr	HU007C1	30.218	33.047	2.829	-0.97	0.98	0.68	0.99
Dublin	IE001C1	22.212	23.891	1.679	-0.78	0.94	0.86	0.95
Roma	IT001C1	29.169	34.38	5.211	-0.52	0.95	0.74	0.99
Milano	IT002C1	30.059	33.856	3.797	-3.50	1.02	0.99	0.98
Napoli	IT003C1	29.774	34.572	4.798	-0.07	0.92	0.85	0.98
Torino	IT004C1	30.082	32.55	2.467	-3.93	1.02	1.09	0.98
Palermo	IT005C1	27.338	36.016	8.678	-2.23	0.94	0.90	0.98
Genova	IT006C1	26.849	33.256	6.407	-3.04	0.99	0.67	0.99
Bari	IT008C1	27.793	33.836	6.043	-0.70	0.94	0.77	0.99
Bologna	IT009C1	27.771	33.866	6.095	-2.00	1.03	0.71	0.99
Trieste	IT015C1	29.776	32.919	3.143	-1.72	1.00	0.67	0.99
Padova	IT028C1	31.631	34.937	3.307	-2.16	1.02	0.83	0.99
Vilnius	LT001C1	26.119	28.811	2.691	-0.47	0.98	0.59	0.99
Klaipėda	LT501C1	26.463	27.966	1.503	-0.52	0.97	0.55	0.99
Luxembourg	LU001C1	26.843	30.187	3.344	-0.88	0.99	0.52	0.99
Rīga	LV001C1	25.291	26.359	1.068	-0.15	0.97	0.43	1.00
Greater Amsterdam	NL002C2	24.888	28.699	3.812	-0.73	0.96	0.77	0.98
Greater Rotterdam	NL003C2	25.525	29.644	4.118	-0.78	0.96	0.77	0.98

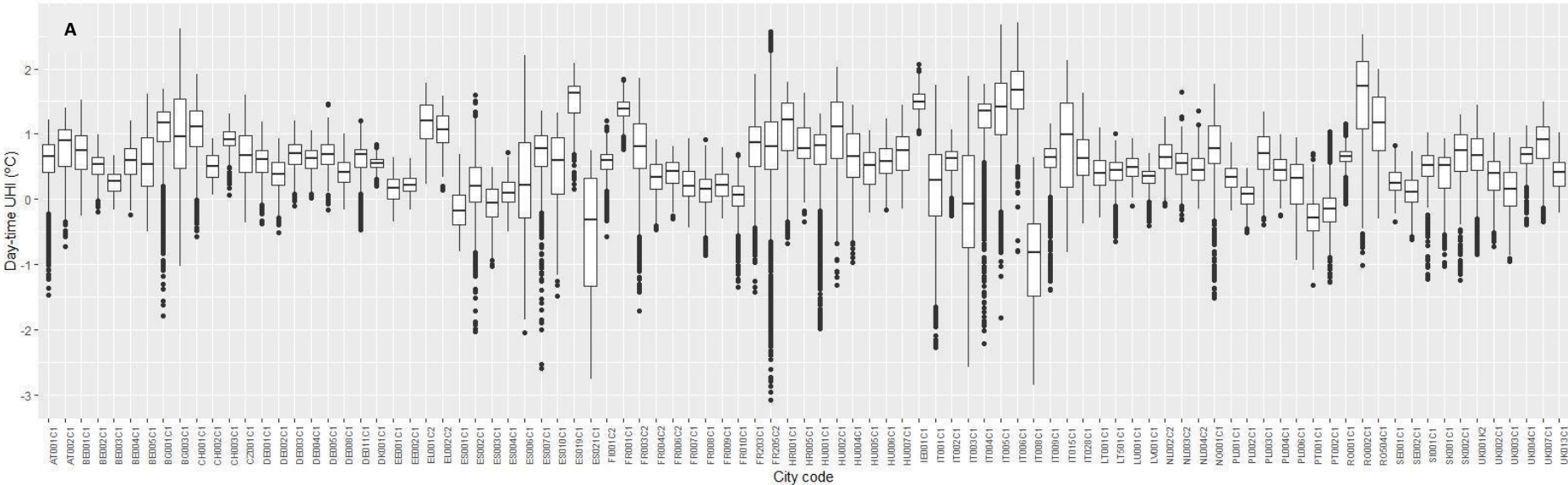
Greater Utrecht	NL004C2	26.183	29.343	3.161	-0.74	0.97	0.80	0.98
Oslo	NO001C1	22.837	23.132	0.294	-2.37	1.05	0.81	0.99
Warszawa	PL001C1	26.733	31.411	4.678	-0.62	0.97	0.58	0.99
Łódź	PL002C1	27.318	30.509	3.192	-0.18	0.97	0.70	0.99
Kraków	PL003C1	24.891	31.403	6.512	-0.94	0.98	0.76	0.99
Wrocław	PL004C1	27.786	32.126	4.34	-0.40	0.98	0.59	0.99
Gdańsk	PL006C1	27.446	29.12	1.675	-0.65	1.00	0.70	0.99
Lisboa	PT001C1	26.688	28.863	2.176	0.22	0.92	0.52	0.98
Porto	PT002C1	28.915	29.236	0.321	-0.25	0.94	0.65	0.98
București	RO001C1	29.772	32.411	2.64	-1.51	0.99	0.93	0.99
Cluj-Napoca	RO002C1	25.328	31.889	6.56	-2.32	0.97	1.06	0.99
Brașov	RO504C1	31.309	29.455	-1.854	-2.91	0.99	0.93	0.99
Stockholm	SE001C1	23.409	25.172	1.763	-0.46	0.97	0.57	0.99
Göteborg	SE002C1	24.863	24.815	-0.048	-0.46	0.97	0.57	0.99
Ljubljana	SI001C1	27.059	31.036	3.977	-2.65	1.02	0.84	0.99
Bratislava	SK001C1	29.355	32.998	3.642	-0.90	1.00	0.62	0.99
Košice	SK002C1	29.3	31.49	2.19	-1.41	1.01	0.64	0.99
London Greater City	UK001K1	21.207	28.2	6.993	-0.87	0.99	0.57	0.98
Birmingham	UK002C1	21.682	26.538	4.856	-0.18	0.97	0.74	0.97
Leeds	UK003C1	21.123	25.804	4.682	-1.09	0.93	0.78	0.96
Glasgow	UK004C1	21.676	24.349	2.673	-1.16	0.96	0.82	0.96
Edinburgh	UK007C1	21.133	24.516	3.383	-0.45	0.95	0.75	0.97
Newcastle upon Tyne	UK013C1	21.031	23.787	2.757	-1.84	0.99	0.73	0.98

Supplement E. Counterfactual scenarios.

a) Urban Heat Island (UHI)

We retrieved the mean day-time UHI and mean night-time UHI data at 100 m x 100 m resolution for 2015 summer season (ie, June - August) from the Copernicus UrbClim model application. This is the difference between the mean rural temperature (ie, represented by the rural classes of CORINE covering grassland, cropland, shrubland, woodland, broadleaf forest and needleleaf forest) and each of the urban grid cells, masking out the water bodies (13).

We estimated the 250m grid cell mean 24hs UHI (ie, for each day) by averaging the day and night UHI 100 m grid cells with centroids within the spatial boundaries of each 250 m grid cell. For the grids with negative values we considered a null UHI. We have also calculated the average daytime and night-time UHI separately to understand the contribution of each to the mean 24hs UHI. Day-time UHI resulted in a mean city value of 0.6°C, whereas night-time UHI was 1.9°C.



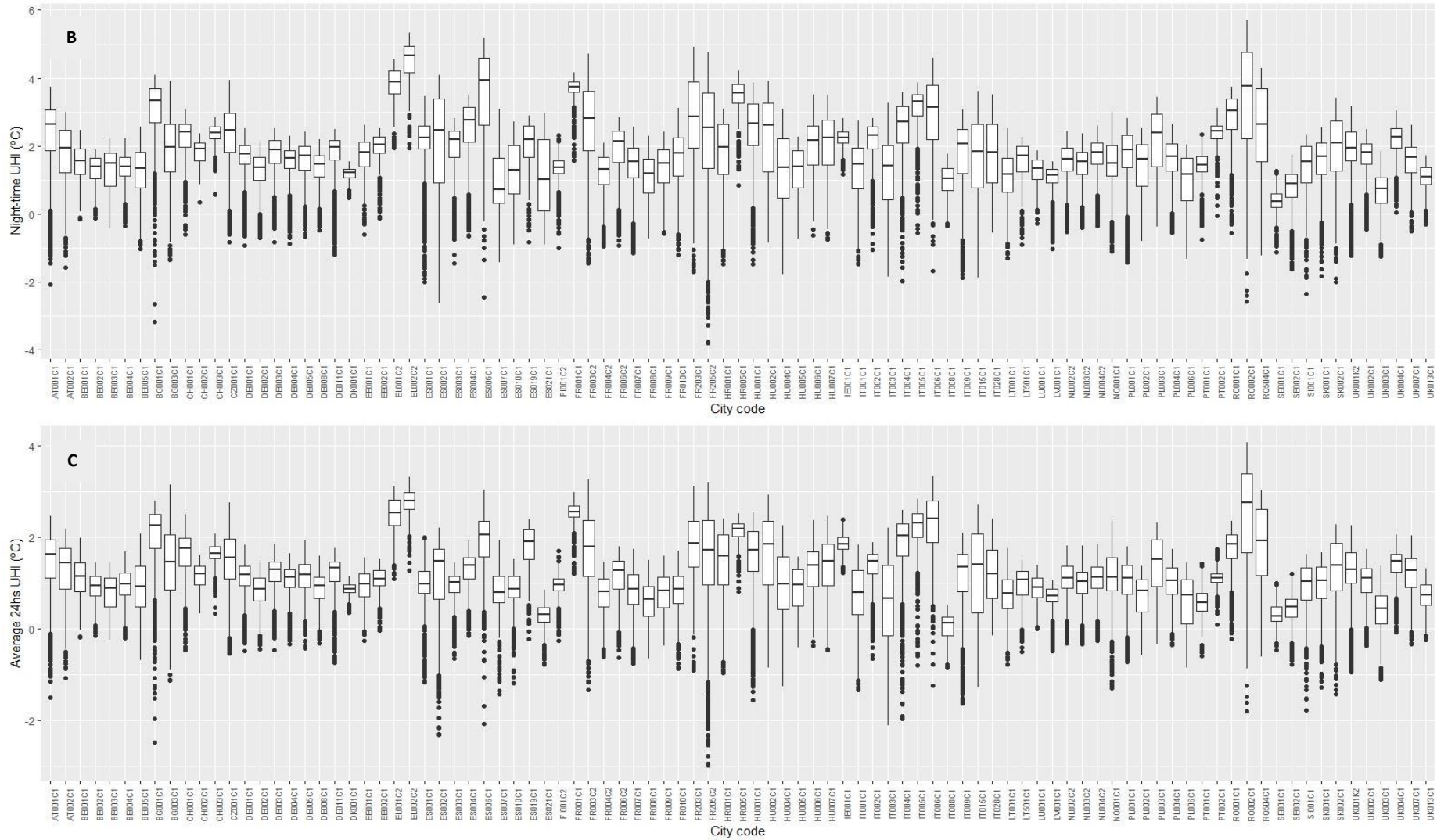


Figure S5. (A) Day-time average urban heat island per grid cell. (B). Night-time average urban heat island per grid cell. (C) 24 hours average urban heat island per grid cell.

Table S4. Distribution of the percentage of negative daily UHI values for day-time (UHId) and night-time (UHIn)

	Minimum (%)	Pct. ¹ 25 (%)	Median (%)	Mean (%)	Pct. ¹ 75 (%)	Maximum
UHId	0.00	5.94	11.67	17.96	23.49	80.07
UHIn	0.00	1.10	3.61	5.07	7.88	22.67

¹. Pct.=percentile

We also estimated the population-weighted city-average by weighting the number of people in a city—divided by the grid—to the UHI exposure in each grid-cell. By summing up all grid-cells estimations, it is possible to have a more accurate measure of the exposure of the city population as it gives proportionately greater weight to the UHI exposure where most people live.

b) TC 30%

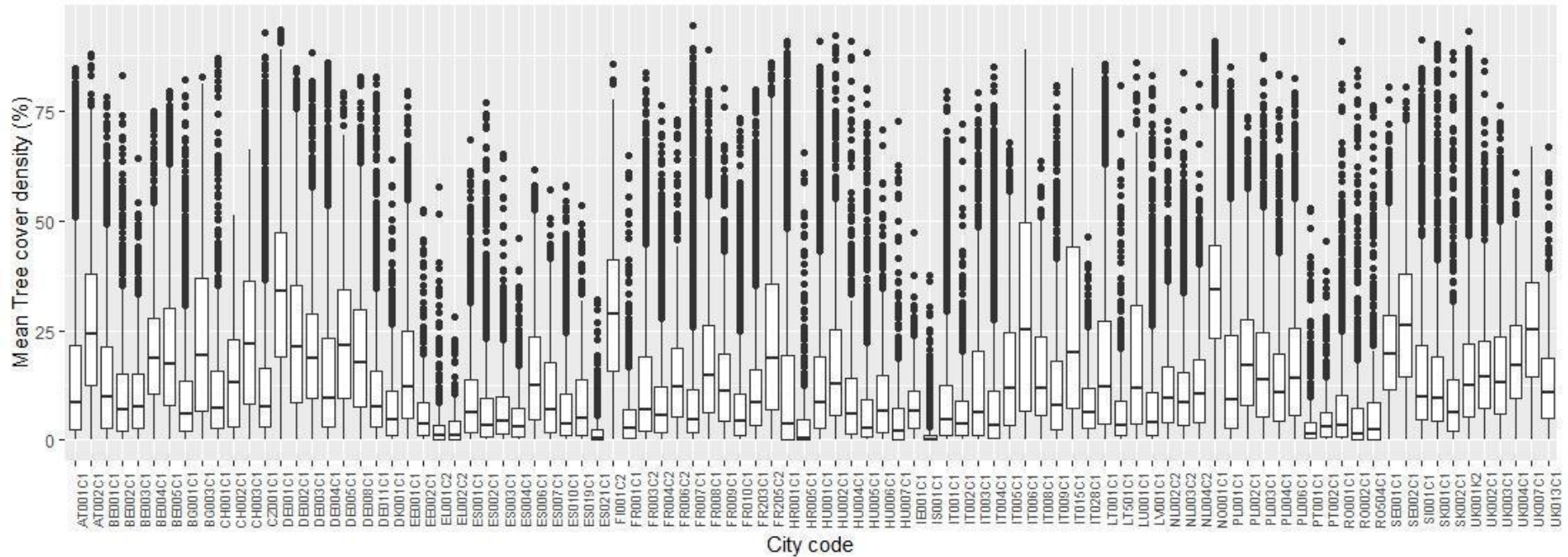


Figure S6. Average tree cover density at a grid cell level by city.

For each city, we analyzed the feasibility of achieving the 30% TC target. We estimated the percentage of open space in each city at a grid cell level where potentially trees could be planted according to the corresponding land use. For this purpose, we retrieved from the European Settlement Map (ESM) the open space (“BU area -open space”) and the green space (“BU - green NDVIx”; green spaces not included in the Urban Atlas (UA) green space classification, such as roadside vegetation, urban trees and pocket parks). We estimated the difference between the 30% target and the available open space at a grid cell level (Figure S7). We calculated the mean and the interquartile range at a city level in order to have the whole picture of the open space distribution (Table S5).

Table S5. Interquartile range of the difference between the 30% TC target and the open space by grid-cell.

City code	Quartile 1	Median	Quartile 3	Mean	City code	Quartile 1	Median	Quartile 3	Mean
AT001C1	0.00	0.00	0.00	2.09	HU001C1	0.00	0.00	0.00	0.91
AT002C1	0.00	0.00	0.00	1.65	HU002C1	0.00	0.00	0.00	2.24
BE001C1	0.00	0.00	12.33	6.18	HU004C1	0.00	0.00	0.00	1.30
BE002C1	0.00	0.00	0.23	2.24	HU005C1	0.00	0.00	0.00	1.80
BE003C1	0.00	0.00	0.85	2.48	HU006C1	0.00	0.00	0.00	1.90
BE004C1	0.00	0.00	0.00	0.52	HU007C1	0.00	0.00	0.94	2.82
BE005C1	0.00	0.00	0.00	1.11	IE001C1	0.00	0.00	0.00	0.12
BG001C1	0.00	0.00	0.00	0.47	IT001C1	0.00	0.00	0.00	1.03
BG003C1	0.00	0.00	0.00	1.07	IT002C1	0.00	0.00	0.00	1.71
CH001C1	0.00	0.00	2.54	2.73	IT003C1	0.00	0.00	0.00	1.05
CH002C1	0.00	0.00	6.23	3.50	IT004C1	0.00	0.00	0.00	1.11
CH003C1	0.00	0.00	5.84	3.68	IT005C1	0.00	0.00	0.00	1.02
CZ001C1	0.00	0.00	0.00	1.37	IT006C1	0.00	0.00	0.00	1.92
DE001C1	0.00	0.00	0.00	1.99	IT008C1	0.00	0.00	0.00	0.95
DE002C1	0.00	0.00	0.00	2.40	IT009C1	0.00	0.00	0.00	1.95
DE003C1	0.00	0.00	0.00	0.71	IT015C1	0.00	0.00	0.00	1.92
DE004C1	0.00	0.00	0.00	1.47	IT028C1	0.00	0.00	0.00	0.53
DE005C1	0.00	0.00	5.91	3.45	LT001C1	0.00	0.00	0.00	1.58
DE008C1	0.00	0.00	0.00	0.76	LT501C1	0.00	0.00	0.00	1.14
DE011C1	0.00	0.00	0.00	1.56	LU001C1	0.00	0.00	1.95	2.74
DK001C1	0.00	2.35	13.48	6.75	LV001C1	0.00	0.00	0.00	1.19
EE001C1	0.00	0.00	0.00	0.41	NL002C2	0.00	0.00	3.53	3.18
EE002C1	0.00	0.00	0.00	0.67	NL003C2	0.00	0.00	5.00	3.33
EL001C2	0.00	0.00	1.69	1.24	NL004C2	0.00	0.00	6.54	3.97
EL002C2	0.00	0.00	0.00	0.35	NO001C1	0.00	0.00	0.00	1.73
ES001C1	0.00	0.00	0.00	1.65	PL001C1	0.00	0.00	0.00	1.02
ES002C1	0.00	0.00	10.46	5.37	PL002C1	0.00	0.00	0.00	1.95

ES003C1	0.00	0.00	0.00	1.98	PL003C1	0.00	0.00	0.00	1.65
ES004C1	0.00	0.00	4.49	3.47	PL004C1	0.00	0.00	0.00	2.16
ES006C1	0.00	0.00	3.18	3.56	PL006C1	0.00	0.00	0.00	1.06
ES007C1	0.00	0.00	0.00	1.47	PT001C1	0.00	0.00	6.46	3.70
ES010C1	0.00	0.00	0.20	2.22	PT002C1	0.00	0.00	0.66	2.05
ES019C1	0.00	0.00	11.06	5.78	RO001C1	0.00	0.00	0.00	1.33
ES021C1	0.00	0.00	0.27	3.46	RO002C1	0.00	0.00	3.42	3.02
FI001C2	0.00	0.00	0.00	0.19	RO504C1	0.00	0.00	4.27	3.98
FR001C1	0.00	6.84	13.01	7.50	SE001C1	0.00	0.00	0.00	1.78
FR003C2	0.00	0.00	0.00	1.62	SE002C1	0.00	0.00	4.12	3.26
FR004C2	0.00	0.00	0.00	1.88	SI001C1	0.00	0.00	5.96	4.17
FR006C2	0.00	0.00	0.00	1.71	SK001C1	0.00	0.00	3.10	2.89
FR007C1	0.00	0.00	0.00	1.55	SK002C1	0.00	0.00	5.46	3.73
FR008C1	0.00	0.00	6.38	3.83	UK001K2	0.00	0.00	0.00	2.85
FR009C1	0.00	0.00	0.56	2.29	UK002C1	0.00	0.00	0.00	1.09
FR010C1	0.00	0.00	3.40	3.20	UK003C1	0.00	0.00	4.94	4.45
FR203C1	0.00	0.00	0.00	2.27	UK004C1	0.00	0.00	0.62	2.78
FR205C2	0.00	0.00	0.00	2.63	UK007C1	0.00	0.00	15.00	7.66
HR001C1	0.00	0.00	0.00	1.90	UK013C1	0.00	0.00	0.00	2.48
HR005C1	0.00	0.00	0.00	0.52					

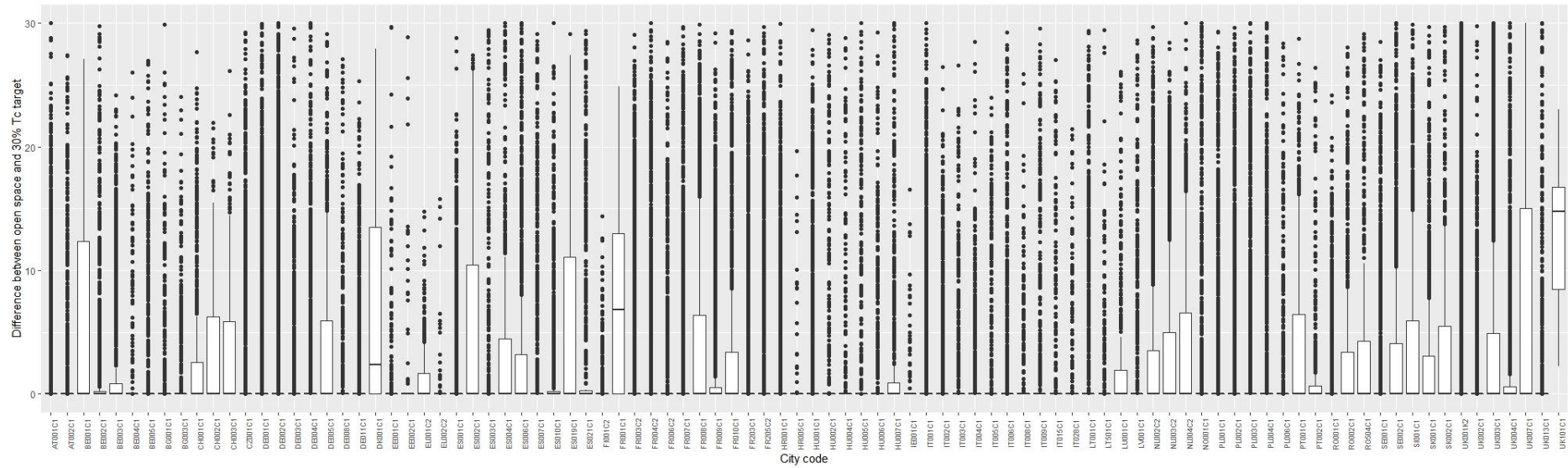


Figure S7. Difference between 30% target and the open space at a grid cell level for each city.

Table S6. Statistical distribution of Equation 2 coefficients and determinant coefficient (R^2)

β_{0e4}	β_{1e4}	β_{2e4}	R^2
36.42 ± 5.50	-0.06 ± 0.003	-1.49 ± 1.01	0.41 ± 0.20

Eq. 2 was built with an US air temperature dataset given that the existing network of weather stations in Europe has insufficient coverage. The dataset, compiled by the University of Colorado Denver, derived from NOAA (National Oceanic and Atmospheric Administration), consists of more than 6,500 summer maximum air temperature records (June 15th to August 15th) from weather stations, including their latitude and the average of 1 km of neighbourhood LST buffer of each station. The wide range of latitudes and biomes covered makes the associations suitable for extrapolation to Europe.

In order to test the model predictions, we used average summer (June–August 2015) air temperature at a city level to validate the air temperature estimated through the model. With this purpose we regressed each city-average value against the corresponding observed air temperature values. We calculated the adjusted R2, RMSE and model coefficients to assess the accuracy of the model.

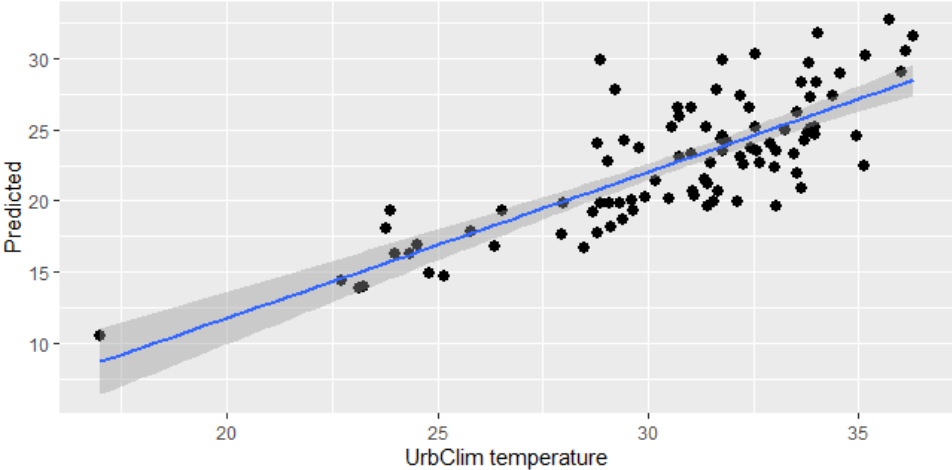


Figure S8. Plot of the cooling model validation. The UrbClim temperature data used in the validation is the average maximum temperature from June to August 2015. Adjusted R2: 0.66; RMSE: 2.03. Both intercept and slope are significant for $p \leq 0.05$.

In order to estimate the LST corresponding to TC equal to 30%, 40% and 25%, we estimated the city-average Etree considering the grid cells with: (1) TC=28-32% (Etree30) and, (2) TC=38-44% (Etree40), (3) TC=23-27% (Etree25), respectively. We considered an interval plus-minus 2^o for avoiding NAs or low counts. For two cities (ie, Thessaloniki, Greece and Murcia, Spain) for which the maximum TC was 30% we computed the same mean evapotranspiration for TC=40%.

Table S7. Distribution of the percentage of negative cooling estimations for TC=30%

	Minimum (%)	Pct. ¹ 25 (%)	Median (%)	Mean (%)	Pct. ¹ 75 (%)	Maximum (%)
Cooling (TC=30%)	0.1	6.63	14.04	16.36	21.82	89.4

¹. Pct.=percentile

Model errors

We estimated the uncertainty of the model by calculating the propagated error of the two regressions, for each city. We applied Eq. S1 based on Taylor et al method for accumulated prediction fractional uncertainties (14).

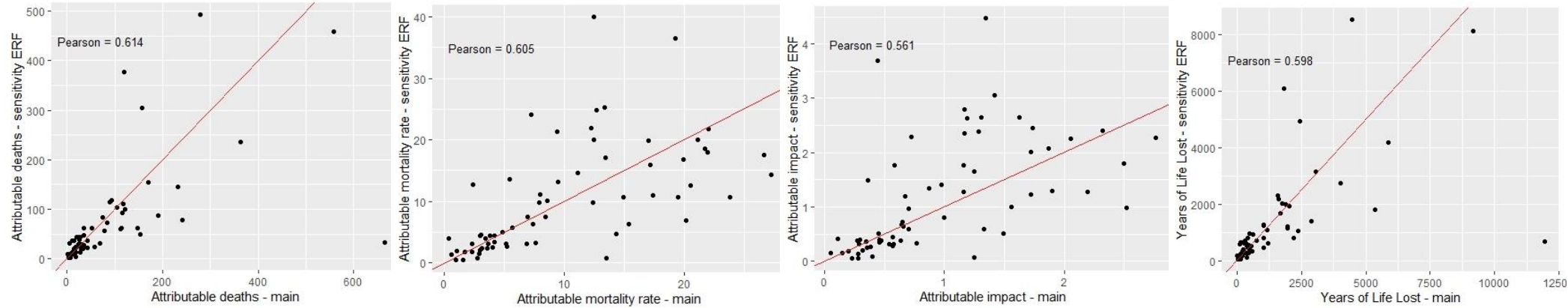
$$\text{(Eq. S4)} \quad \text{Error} = \sqrt{(\delta T_a / |T_a|)^2 + (\delta LST / |LST|)^2 + (\delta T_{a30} / |T_{a30}|)^2 + (\delta LST_{30} / |LST_{30}|)^2}$$

Where δ is the error, T_a is the estimated air temperature, LST is the land surface temperature, and T_{a30} and LST_{30} are the estimated air and surface temperature for TC=30% scenario, respectively. We calculated the errors (δ) by averaging the observed upper and lower confidence interval ($\alpha = 0.05$) values from grid- cell-level predictions,

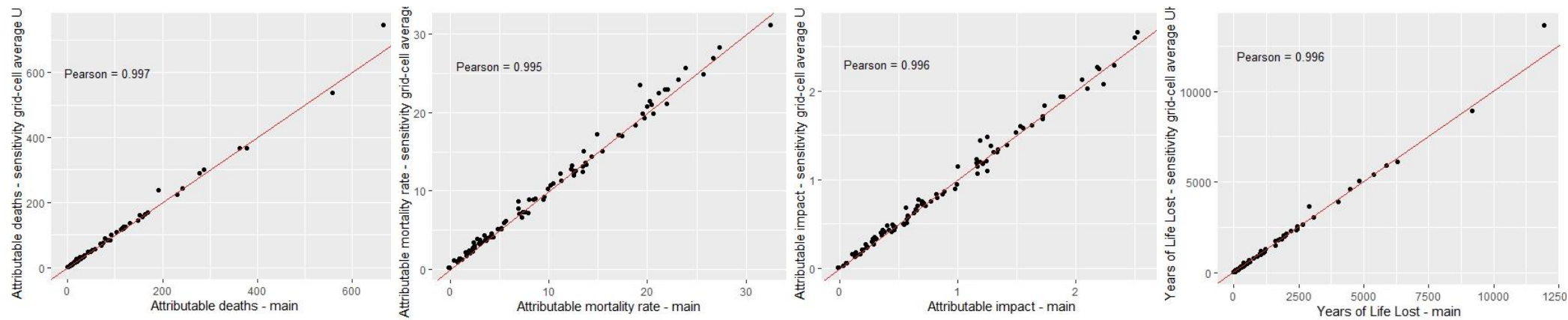
Supplementary F. Sensitivity analysis.

a) Health impact assessment of urban heat island

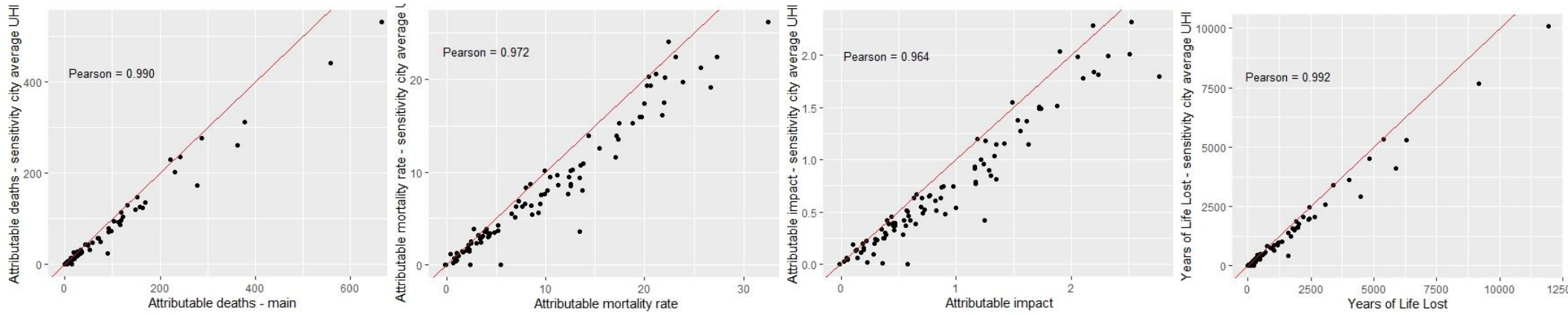
i) Exposure response function (Martinez-Solanas et al, 2021)



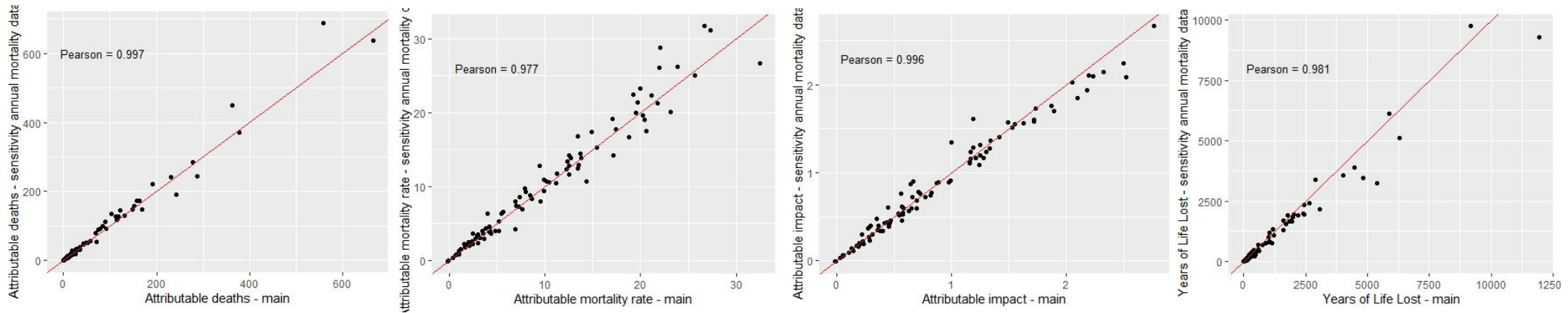
ii) Grid-cell-average summer UHI



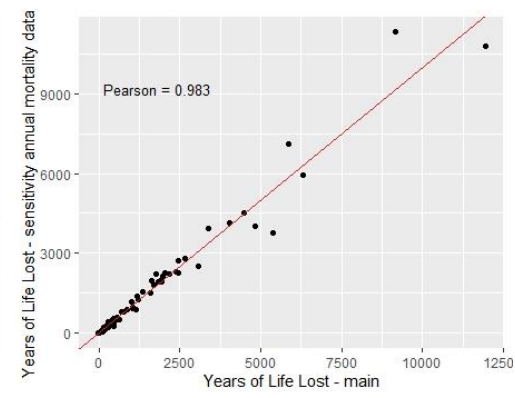
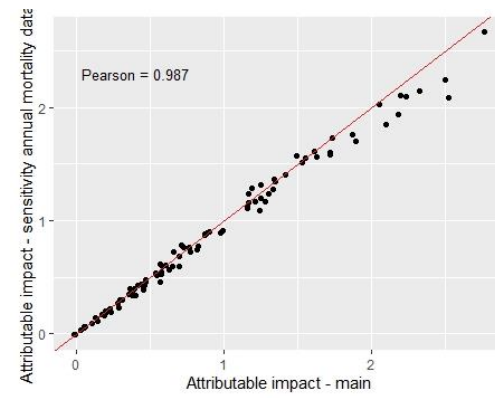
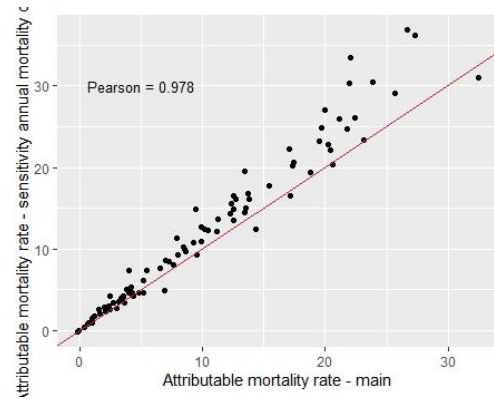
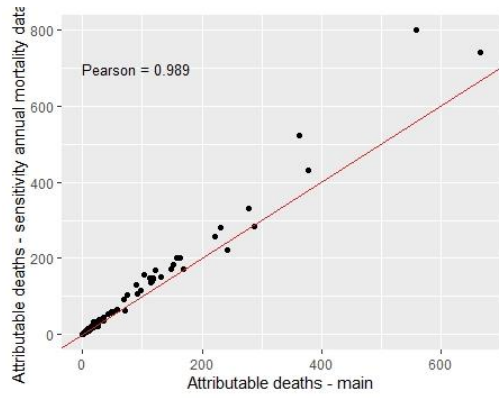
iii) City-average UHI



iv) Adjusted annual city mortality dataset



v) Non-adjusted annual city mortality dataset



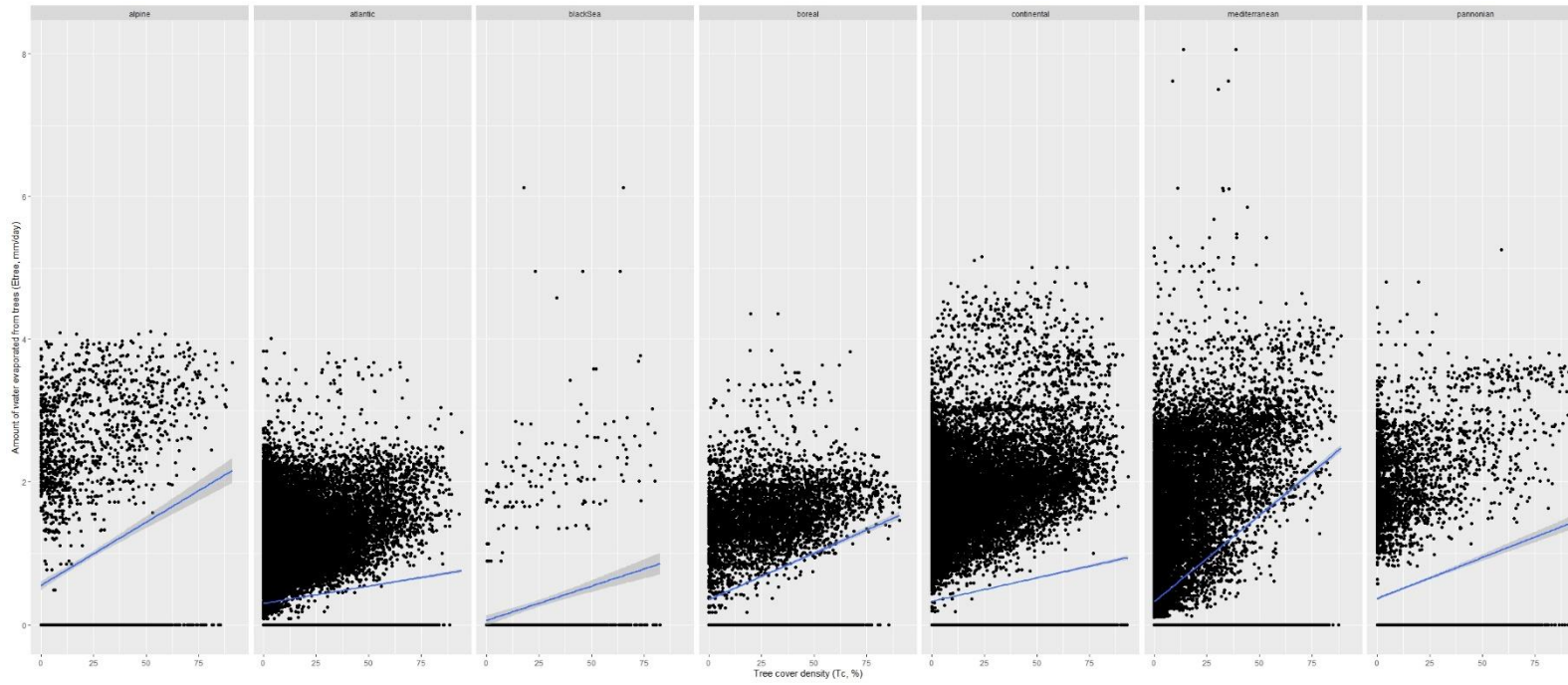
b) Cooling estimation

We conducted two sensitivity analysis of the cooling estimation for TC=30% changing the way the amount of water evaporated from trees (E_{tree30}) was calculated.

1) Linear regressions by city between the TC and E_{tree}

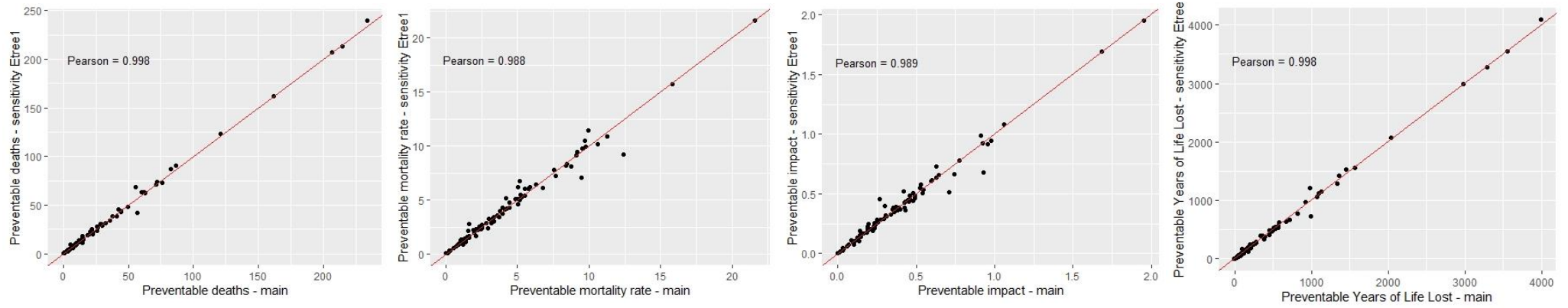


2) Linear regression by biome between the TC and E_{tree}

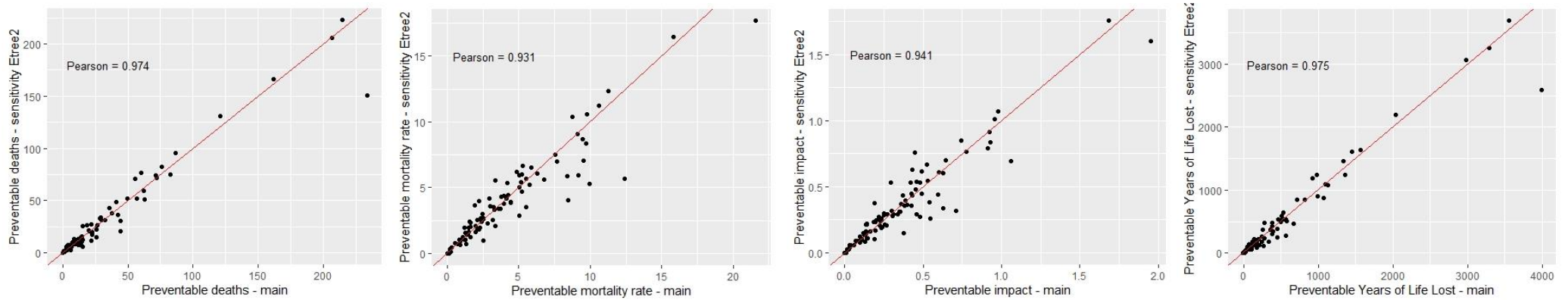


c) 30% TC health impact assessment

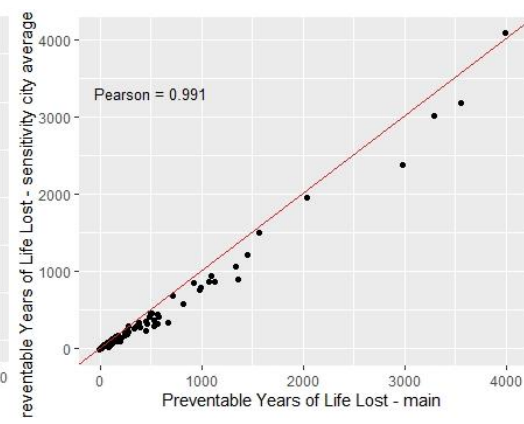
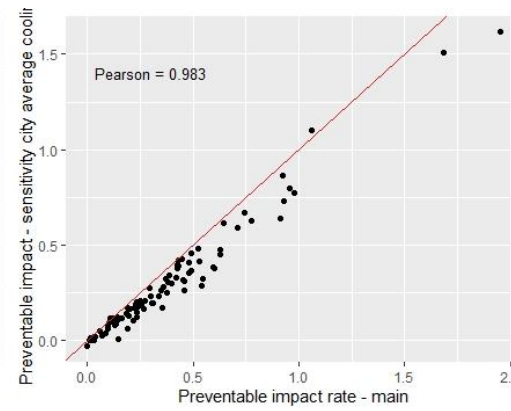
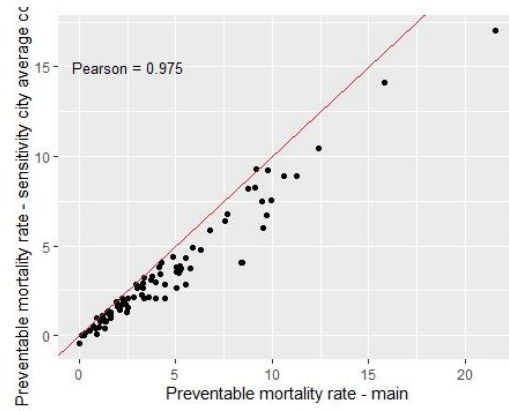
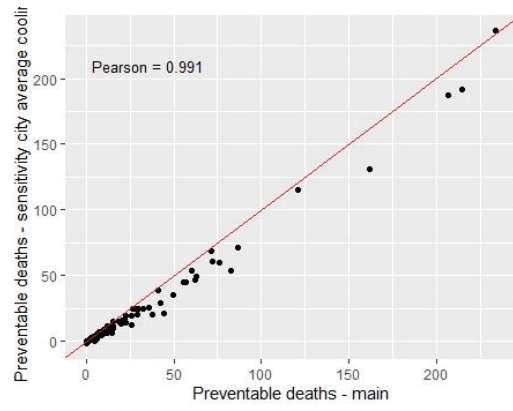
i) Etree₃₀ estimation: regression by city



ii) Etree₃₀ estimation: linear regression by biome



iii) City-average cooling



iv) Exposure response function (Martinez-Solanas et al, 2021)

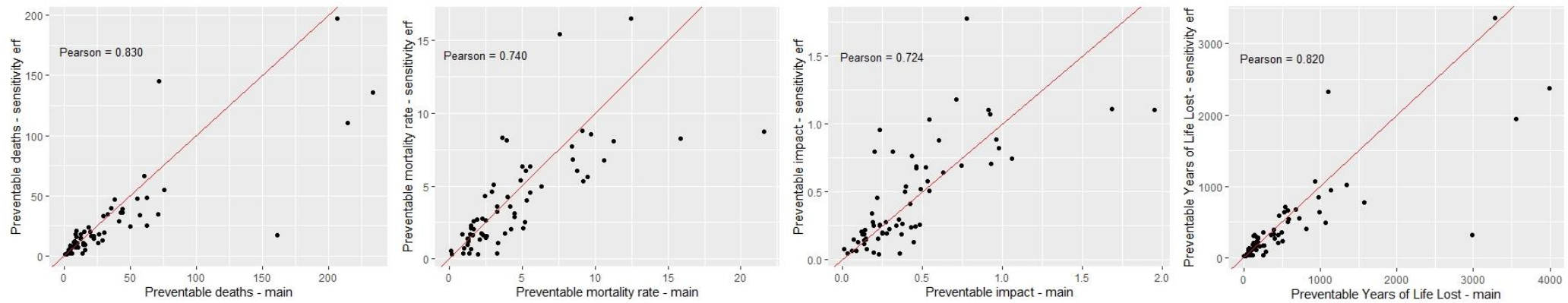
We applied the same methodology than for the main analysis.

Given that the risk estimates were built under the E-obs dataset (15), we applied a city-specific correction to the UrbClim dataset as:

$$\text{Eq. (S5)} \quad T_{\text{urbclim}} = \alpha + \beta_3 * T_{\text{E-obs}}$$

Where T_{urbclim} is the mean UrbClim daily city-level temperature and $T_{\text{E-obs}}$ is the mean E-obs daily city-level temperature for 2015.

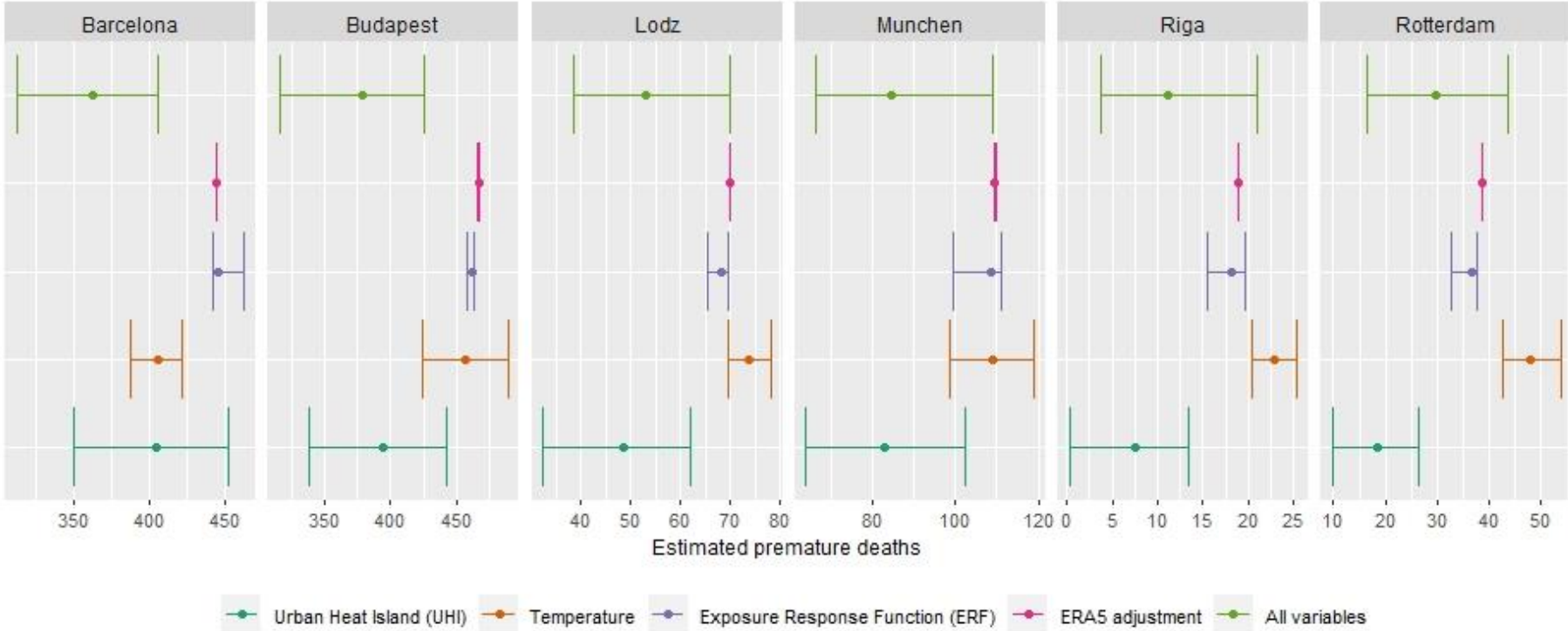
After adjusting the temperature dataset, there were still some days with temperature values falling out of the ERFs (ie, temperature values above the maximum temperature with an estimated risk). We chose a conservative approach and instead of extrapolating the ERFs above the maximum, we assigned to highest temperatures, the corresponding maximum temperature' risk available.



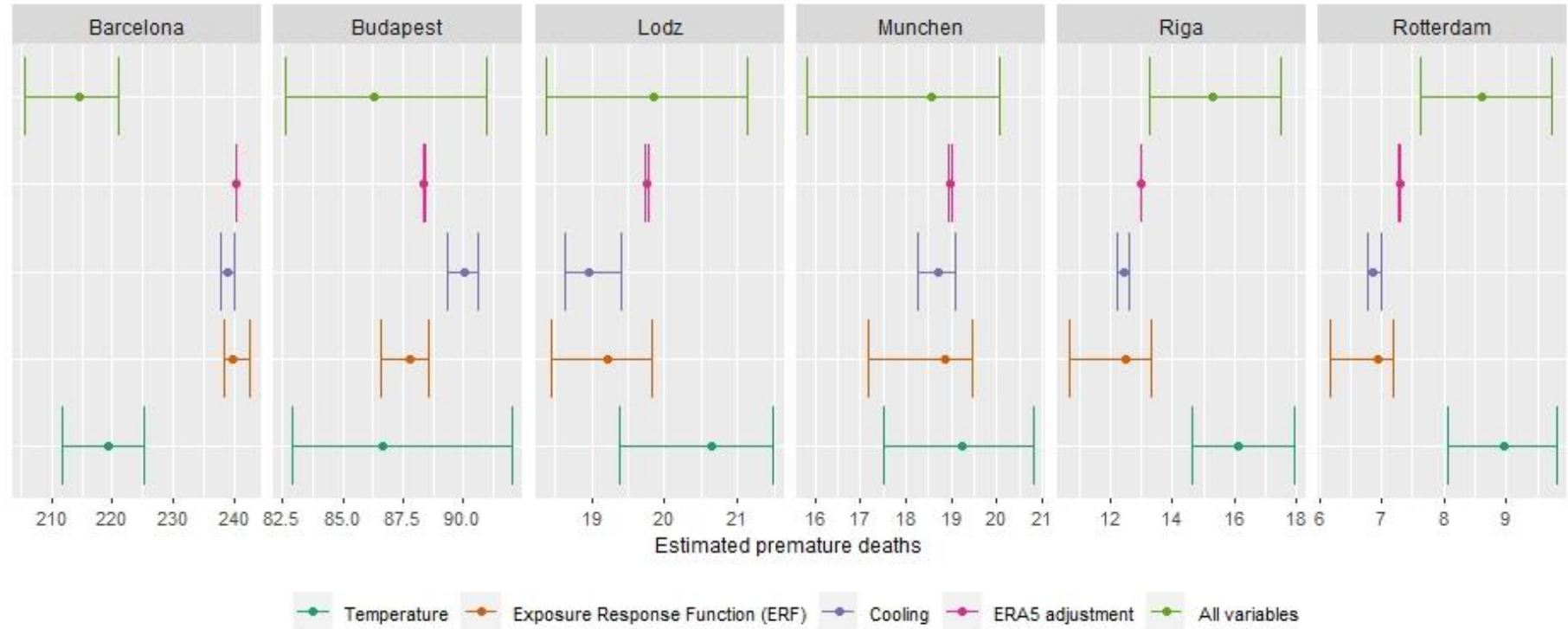
Supplementary analysis G. Uncertainty analyses.

We conducted uncertainty analysis running 500 Monte Carlo simulations considering each of the parameter's uncertainty separately. We considered the following sources of uncertainties: the ERFs (8), the UrbClim data error (16), the temperature adjustment model error, the UHI data error (16) and the cooling model error, accordingly.

- Urban heat island health impact assessment



- 30% TC scenario health impact assessment



References

1. Eurostat. Urban Audit. 2018; Available from: <https://ec.europa.eu/eurostat/web/cities/data/database>
2. Dijkstra, L. & Poelman H. Cities in Europe. The new OECD-EC definition. 2012;
3. European Commission. Global Human Settlement [Internet]. 2019 [cited 2021 Sep 14]. Available from: <https://ghsl.jrc.ec.europa.eu/data.php>
4. Copernicus. Urban Atlas 2012. 2012.
5. Eurostat. Regional statistics by NUTS classification. 2019.
6. Eurostat. NUTS - NOMENCLATURE OF TERRITORIAL UNITS FOR STATISTICS. 2018.
7. Eurostat. Database [Internet]. [cited 2021 Dec 27]. Available from: <https://ec.europa.eu/eurostat/data/database>
8. Masselot P. Excess mortality attributed to heat and cold in 801 cities in Europe. Forthcoming.
9. Lee W, Kim H, Hwang S, Zanobetti A, Schwartz JD, Chung Y. Monte Carlo simulation-based estimation for the minimum mortality temperature in temperature-mortality association study. *BMC Med Res Methodol*. 2017;17(1):1–10.
10. Eurostat. Revision of the European Standard Population. Report of Eurostat’s task force. 2013.
11. Eurostat. Life expectancy at birth by sex [Internet]. [cited 2021 Nov 10]. Available from: <https://ec.europa.eu/eurostat/databrowser/view/tps00205/default/table?lang=en>
12. WHO. WHO methods and data sources for global burden of disease estimates 2000-2011. 2013;(November):86. Available from: http://www.who.int/healthinfo/statistics/GlobalDALYmethods_2000_2011.pdf?ua=1
13. Copernicus. Corine Land Cover [Internet]. 2012 [cited 2021 Sep 3]. Available from: <https://land.copernicus.eu/pan-european/corine-land-cover>
14. Taylor J. Introduction to Error Analysis, the Study of Uncertainties in Physical Measurements, 2nd Edition. 1997.
15. European Climate Assessment & Dataset project. E-OBS gridded dataset [Internet]. [cited 2021 Nov 15]. Available from: <https://www.ecad.eu/download/ensembles/download.php>
16. De Ridder K, Lauwaet D, Maiheu B. UrbClim – A fast urban boundary layer climate model. *Urban Clim* [Internet]. 2015 Jun 1 [cited 2020 Mar

19];12:21–48. Available from: <https://www.sciencedirect.com/science/article/abs/pii/S2212095515000024?via%3Dihub>